Domain Wall Orientation in Magnetic Nanowires

E. Y. Vedmedenko,[1,2] A. Kubetzka,[2] K. von Bergmann,[2] O. Pietzsch,[2] M. Bode,[2] J. Kirschner,[1]
H. P. Oepen,[2] and R. Wiesendanger[2]

[1]*Max-Planck-Institut für Mikrostrukturphysik, Weinberg 2, D-06120 Halle, Germany*
[2]*Institute of Applied Physics, University of Hamburg, Jungiusstrasse 11, D-20355 Hamburg, Germany*
(Received 31 July 2003; published 20 February 2004)

Scanning tunneling microscopy reveals that domain walls in ultrathin Fe nanowires are oriented along a certain crystallographic direction, regardless of the orientation of the wires. Monte Carlo simulations on a discrete lattice are in accordance with the experiment if the film relaxation is taken into account. We demonstrate that the wall orientation is determined by the atomic lattice and the resulting strength of an effective exchange interaction. The magnetic anisotropy and the magnetostatic energy play a minor role for the wall orientation in that system.

Magnetism of systems with reduced dimensions poses a number of topical questions, one intriguing issue being the orientation of domain walls. It has been shown experimentally that the mesoscopic pathway of domain walls in ultrathin films can either be arbitrary, as in Co/Au(111) [1], or follow certain crystallographic directions, as in Fe/W(110) [2]. Although the knowledge of domain patterns and, in particular, the domain wall orientation on the nanoscale is of great importance for the fundamental physics of magnetism, as well as for technical applications, the orientation of domain walls on a local, microscopic scale has not yet been studied.

One experimentally accessible and, for future applications, very perspective geometrical shape is a so-called nanowire—a quasi-one-dimensional structure of infinite length and lateral dimensions on the nanometer scale. The nanowire geometry is particularly advantageous for the investigation of the domain wall orientation as the latter can be governed by a minimization of the total wall length. On the other hand, it has been demonstrated that in ultrathin nanostructures the discreteness of the crystalline lattice can also change the magnetization configuration [3]. The role of the lattice for the domain wall orientation has not been analyzed systematically.

For many experimental systems, e.g., Fe/Cu(100), the shortest wall path coincides with one of the crystallographic axes which makes it impossible to distinguish between the role of the lattice for the domain formation and other effects. Only if the shortest distance is different from any principal axes of a lattice the mechanism underlying the orientation of the domain walls can be revealed. A suitable and experimentally well-studied model system is the double layer (DL) Fe nanowires on stepped W(110) [2,4–8] being characterized by perpendicularly magnetized domains separated by domain walls. Experimental and *ab initio* electronic structure calculations [9] led to a comprehensive understanding of the electronic and the magnetic properties. The relationship between the orientation of domain walls and of the DL Fe stripes, however, has not yet been investigated.

This study is devoted to the analysis of the influence of the discrete nature of an atomic lattice on the orientation of domain walls in nanostructures. Scanning tunneling microscopy on areas with different local miscut orientations reveals that the domain walls are oriented along the $[1\bar{1}0]$ and less often along the $[3\bar{3}1]$ direction, regardless of the orientation of the nanowires. Employing Monte Carlo simulations (MCS) we demonstrate that the wall orientation is determined by the underlying crystalline lattice and the exchange interactions. The magnetic anisotropy and the magnetostatic energy, which can align walls along certain crystallographic directions in bulk material, play a minor role for the wall orientation. We regard these results to be valid for a large class of low symmetry ultrathin ferromagnetic films.

The experiments have been performed in a commercial variable temperature STM attached to a five-chamber UHV system. The instrument is equipped with an *x-y* sample positioning facility which allows one to access different areas on the same sample. We used etched tungsten tips for the measurements. Fe was deposited onto the W(110) substrate by molecular beam epitaxy at a pressure $p \leq 1 \times 10^{-10}$ mbar. To achieve step flow growth the crystal was held at $T = 500$ K during thin film deposition. Simultaneously to constant current images, maps of the differential conductance dI/dU were recorded by means of the lock-in technique.

Figure 1 shows the topography (a) and maps of differential conductance (b)–(d) of 1.7 ML (monolayer) Fe/W(110). While the dI/dU map of Fig. 1(b) has been measured simultaneously with and at the same position as the topographic image, the dI/dU maps of Figs. 1(c) and 1(d) show other areas of the same sample which exhibit different local miscut orientations. In any case the Fe DL nanowires can be distinguished from sample locations which are covered by a single Fe layer (SL) due to their different electronic properties resulting in a dI/dU signal that is lower for the SL than for the DL. The DL nanowires shown in Figs. 1(a) and 1(b) extend approximately along [001], the ones in Fig. 1(c) along $[1\bar{1}0]$, while in
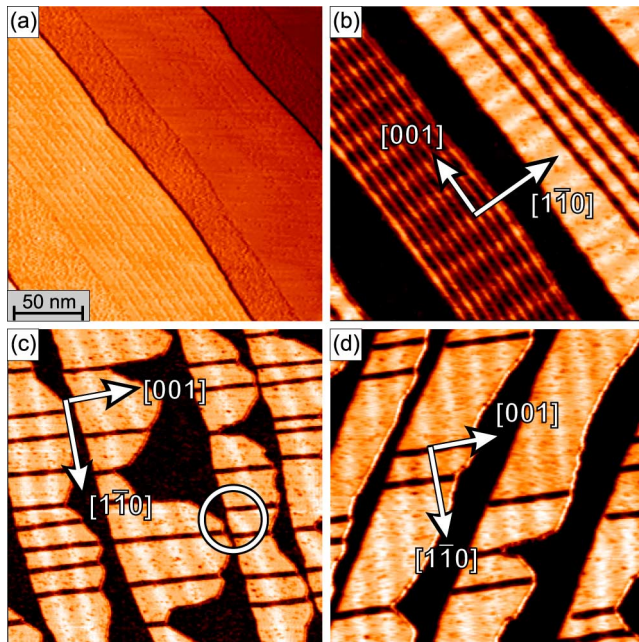
FIG. 1 (color online). (a) Topography and (b)–(d) dI/dU maps of 1.7 ML Fe/W(110) at different local miscut orientation. (a) and (b) were recorded simultaneously. The lateral scale is the same in all images. In all cases, domain walls (white lines) are oriented along $[1\bar{1}0]$, regardless of the orientation of the nanowires. Parameters are $U = 5$ mV, $I = 0.5$ nA, $T = 75$ K (b),(c), and 120 K (d).

FIG. 2 (color online). Top view of experimental (a) and simulated nanowire sections of 20 nm (b)–(d) and 40 nm widths (e): (a) experiment, domain walls are imaged as dark lines; (b) continuum theory, isotropic exchange. MCS: (c) $J_3:J_2:J_1 = 0:1:1$ (identical exchange interaction along all nearest neighbor bonds); (d),(e) $J_3:J_2:J_1 = 4:2:1$.

Fig. 1(d) the wire direction is intermediate, roughly along $[1\bar{1}1]$. Because of unequal diffusion energies the Fe stripes grow smoothest along [001] and least smooth along $[1\bar{1}0]$ [10]. After initial pseudomorphic growth the high tensile strain starts to relax by insertion of dislocation lines in the Fe DL which run along the [001] direction. These are imaged as narrow black lines in the dI/dU maps. The double layer nanowire has a periodic magnetic structure with out-of-plane domains alternatingly magnetized up and down. These domains are separated by 180° in-plane domain walls. The typical distance between adjacent walls is 23 ± 2 nm [8]. Because of spin-orbit coupling we can differentiate between areas with out-of-plane and in-plane magnetization even with nonmagnetic tips [4]. Since the bias voltage chosen for the measurements of Fig. 1 ($U = 5$ mV) is below the crossover of domain and domain wall spectra [see Fig. 1(e) in Ref. [4]] the domain walls are imaged as white lines in this experiment. Regardless of the direction of the nanowires the domain walls run mainly along the $[1\bar{1}0]$ direction, i.e., perpendicular to the dislocation lines. As a consequence, the domain walls within the nanowires are infinitely long in the case of Fig. 1(c)(disregarding interruptions due to structural imperfections), and very short in case of Fig. 1(b) where they run perpendicular to the axis of the nanowire. Less often the domain walls run along $[3\bar{3}1]$. This effect can be seen in Fig. 2(a) where a DL, 20 nm wide nanowire is shown. As the bias voltage

and the material of the STM tip were different from those of experiment Fig. 1 the domain walls are imaged as dark lines [2]. Both $[1\bar{1}0]$ and $[3\bar{3}1]$ directions are not principal directions of an ideal bcc lattice as they do not coincide with the primitive vectors of the bcc structure.

We have performed calculations following a widely used micromagnetic framework [11], where the nanowires consist of rectangular blocks of continuous material. For isotropic exchange stiffness A we obtain the wall direction that is determined by a minimization of the wall length, i.e., perpendicular to the nanowire direction [Fig. 2(b)]. This result is not consistent with the experimental observation of Fig. 1. It even cannot be corrected by an additional in-plane anisotropy [Fig. 2(b)]; this leads only to an alignment of the magnetization within the wall with no consequences for the wall direction. Varying A in the $[1\bar{1}0]$ and in the [001] direction [12], we obtain a tilting of the domain wall [13]. Hence, in contrast to bulk materials where magnetic anisotropy may affect the wall direction, the exchange stiffness plays a more important role in the ultrathin limit. The anisotropy of the continuum parameter A can be governed either by noncubic symmetry of the lattice or by the varying exchange integral between nearest-neighboring atoms [12]. By fitting A to the experimental results we cannot distinguish between the two effects. Besides, we cannot explain the experimental observation of coexisting $[1\bar{1}0]$ and $[3\bar{3}1]$ walls. Thus, without consideration of the discrete atomic lattice the physics of the wall orientation in the ultrathin limit cannot be understood.

In order to explain the experimental results we performed MCS on a discrete lattice. In contrast to the case of localized spin systems, in itinerant-electron systems the exchange coupling between local moments does not explicitly enter into a Heisenberg-type Hamiltonian. However, within the framework of spin-density-functional theory expressions for the effective exchange pair interactions can be obtained [14,15]. With these effective constants the system Hamiltonian for the MC calculations reads

$$H = -\sum_{\langle i,j \rangle} J_k \boldsymbol{S}_i \cdot \boldsymbol{S}_j + D\sum_{i,j}\left(\frac{\boldsymbol{S}_i \cdot \boldsymbol{S}_j}{r_{ij}^3} - 3\frac{(\boldsymbol{S}_i \cdot \boldsymbol{r}_{ij})(\boldsymbol{S}_j \cdot \boldsymbol{r}_{ij})}{r_{ij}^5}\right) + k_1\sum_i \sin^2\theta + k_2\sum_i \sin^4\theta - k_p\sum_i \sin^2\theta\cos^2(\varphi - \beta),$$

where J_k denotes the effective nearest neighbor exchange coupling constant along different bonds (Fig. 3), D is the dipolar coupling parameter, θ and φ are the spherical angles, and $\boldsymbol{r}_{ij}$ is the vector between sites i and j. The coefficients k_1 and k_2 are the first- and second-order anisotropies per atom, respectively. k_p is an in-plane anisotropy per atom. The in-plane anisotropy can have any angle β with respect to the x axis. For the MC computations we consider two layers of classical, three-dimensional magnetic moments $\boldsymbol{S}$ on a bcc(110) lattice of about 20 000 effective magnetic sites. The Monte Carlo procedure is described elsewhere [16]. We use a realistic ratio of exchange and dipolar constants $D/J = 10^{-3}$. The anisotropy constants have been widely varied in the regime of the vertical magnetization. The best agreement with the experimental results (domain width of 20–25 nm and wall width of 6–9 nm) gives constants corresponding to an anisotropy energy density $K_1 = (1.6–2.0)K_d$, $K_2 = (0–0.7)K_d$, $K_p = (0–0.6)K_d$ with $K_d = 2\pi M_s^2$ the shape anisotropy. The value of the out-of-plane anisotropy is $K_1 = (2–2.1)K_d$. We have performed calculations for films, single wires, and arrays of three wires with periodic boundary conditions along the wires and open boundary conditions in the perpendicular direction.

In a first step we assume an idealized film with an "isotropic" nearest neighbor exchange, i.e., $J_1 = J_2$ and $J_3 = 0$ in the case of a bcc(110) lattice (cf. Fig. 3). In infinite sc(100) or an fcc(111) 1–2 ML films no preferred wall orientation is observed. In contrast, domain walls in a 2 ML bcc(110) film have mainly $[1\bar{1}0]$ orientation. This can be explained by the minimization of the density of
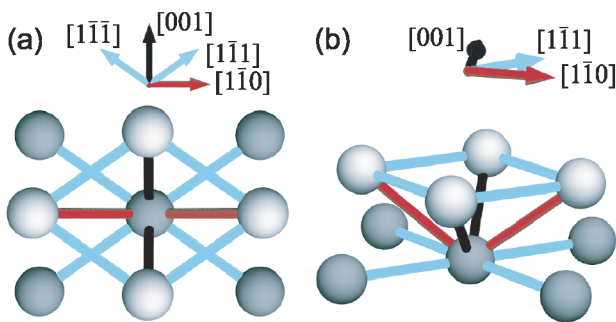
nearest neighbor bonds per unit volume of a wall for this direction. As a consequence, the exchange energy cost due to the wall formation can be minimized. The same results have been obtained for wide wires (>40 nm). Those results are consistent with experiments and demonstrate that the crystal lattice can affect the wall orientation.

A typical result for the case of $[1\bar{1}\,\bar{1}]$ oriented, 20 nm wide nanowires is given in Fig. 2(c). In that case the walls deviate from the $[1\bar{1}0]$ direction. The orientation of walls is close to $[1\bar{1}1]$. Hence, the lattice symmetry alone is insufficient to orient the domain walls along $[1\bar{1}0]$. The calculations show that if the length of the walls can be minimized as, for example, in thin wires of Fig. 2(c) the wall orientation can deviate from $[1\bar{1}0]$. In the following we explain the discrepancy by taking into account the lattice relaxation.

Because of pseudomorphic growth the first two Fe layers adopt the lateral lattice constant of tungsten, which is about 10% larger than that of bulk iron. As a consequence, the Fe-Fe interlayer distance relaxes below the Fe bulk value [9]. This leads to a change of the interatomic distances. Namely, the neighbor distance in the [001] direction (black in Fig. 3) d_1 decreases, the spacings in the $[1\bar{1}1]$ and the $[1\bar{1}\,\bar{1}]$ direction d_2 (light grey) are increased, and the distance in the $[1\bar{1}0]$ d_3 direction (dark grey) decreases to a value close to the nearest neighbor distance in bulk iron. Hence, instead of six nearest neighbors as in an ideal, 2 ML thick bcc(110) film, in Fe/W(110) all atoms have eighth bonds of similar length. The respective distances in units of the nearest neighbor distance in bulk Fe are $d_1 = 0.82$, $d_2 = 0.96$, and $d_3 = 0.99$ [9].

The calculations [14,17–19] show that the strength of the exchange coupling is a function of relative position $\boldsymbol{r}_{ij}$ of the magnetic moments i and j. Especially interesting is the behavior of $J(\boldsymbol{r}_{ij})$ in Fe. For Fe a reduction in nearest neighbor (NN) spacing d_{NN} with respect to the bulk value drives the exchange towards antiferromagnetism. This effect has been made responsible for the fact that fcc-Fe is antiferromagnetic while bcc-Fe is a ferromagnetic material [20,21]. That argument is also supported by the position of Fe on the Bethe-Slater curve, which is widely used in the physics of ferromagnetic alloys [21,22]. Thus, a decrease of the interatomic distance in the [001] direction can lead — in contrast to other ferromagnets — to a reduction of the ferromagnetic exchange parameter.

FIG. 3 (color online). Unit cell of 2 ML Fe/W(110) in (a) top and (b) perspective views. Black and light grey (blue) lines denote the nearest neighboring bonds J_1 and J_2 in an undistorted, ideal crystal. Dark grey (red) lines denote additional nearest neighboring bonds J_3 due to relaxation.

For Fe nanowires on W(110) the situation is even more subtle due to hybridization and polarization effects at the Fe/W interface. All the more interesting is the advance, described in very recent studies [23,24], where the exchange stiffness of Fe films adsorbed on a W(110) surface has been calculated. The authors find that the exchange stiffness A, which is equal to $2JS^2/a$ for a bcc lattice [25], depends on the direction along which the spin wave is excited. For one monolayer Fe/W(110) the exchange stiffness in the $[1\bar{1}0]$ direction is 4 times larger than in the [001] direction [24]. For a 2 ML film the difference is found to be smaller, but the tendency remains the same. The physical reason for this anisotropic behavior can lie in changes of interatomic spacing, as discussed above, or in additional indirect spin interactions through the W substrate [24]. In any case, the dependence of the exchange interaction on r_{ij} must be taken into account in the simulation of the magnetic ordering.

According to this argument we introduce three different exchange constants J_i for the three nonequivalent pairs of neighboring magnetic moments. Hamiltonians of that type are widely used in models of frustrated magnetic systems [26]. We have explored different ratios of $J_3:J_2:J_1$ (dark grey, light grey, and black bonds in Fig. 3, respectively). Generally, the walls tend to be aligned along the axis of the strongest exchange coupling. The best overall accordance with the experiment is found for ratio $J_3:J_2:J_1 = 4:2:1$, which is in good agreement with Refs. [23,24] and the Bethe-Slater curve. For $[1\bar{1}1]$ nanowires [Fig. 2(d)] the majority of the walls follow the $[1\bar{1}0]$ axis. However, $[3\bar{3}1]$ walls are also found. For $[1\bar{1}0]$ nanowires of 40 nm width [Fig. 2(e)] we also get $[1\bar{1}0]$ oriented domain walls which cannot be expected from isotropic exchange interactions. The walls are not perfectly straight but show some irregularities. For example, the wall is forced out of the $[1\bar{1}0]$ direction at the rim of the nanowire. A similar behavior has also been found experimentally [see the circle in Fig. 1(c)]. We have also explored different orientations and strengths of the in-plane anisotropy K_p. As already mentioned above the only effect of a strong K_p is an alignment of the magnetic moments in the wall along the respective axis. The orientation of domain walls is not influenced by K_p showing that the mechanism of wall orientation described here is distinct from the one observed in bulk material, which is governed by magnetic anisotropy and dipolar energy.

In conclusion, we have demonstrated by means of an experimental study and extended Monte Carlo simulations that in contradiction to the isotropic continuum approximation the orientation of magnetic domain walls in ultrathin films is governed by the atomic lattice structure and the set of nearest neighbor moments. The magnetic anisotropy and the magnetostatic energy, which can govern wall orientations in bulk material, play a minor role in the ultrathin limit.

[1] M. Speckmann, H. Oepen, and H. Ibach, Phys. Rev. Lett. **75**, 2035 (1995).

[2] A. Kubetzka, M. Bode, O. Pietzsch, and R. Wiesendanger, Phys. Rev. Lett. **88**, 057201 (2002).

[3] E. Vedmedenko, H. Oepen, and J. Kirschner, J. Magn. Magn. Mater. **256**, 237 (2003).

[4] M. Bode, S. Heinze, A. Kubetzka, O. Pietzsch, X. Nie, G. Bihlmayer, S. Blügel, and R. Wiesendanger, Phys. Rev. Lett. **89**, 237205 (2002).

[5] M. Bode, A. Kubetzka, S. Heinze, O. Pietzsch, R. Wiesendanger, M. Heide, X. Nie, G. Bihlmayer, and S. Blügel, J. Phys. Condens. Matter **15**, S679 (2003).

[6] O. Pietzsch, A. Kubetzka, M. Bode, and R. Wiesendanger, Science **292**, 2053 (2001).

[7] O. Pietzsch, A. Kubetzka, M. Bode, and R. Wiesendanger, Phys. Rev. Lett. **84**, 5212 (2000).

[8] A. Kubetzka, O. Pietzsch, M. Bode, and R. Wiesendanger, Phys. Rev. B **67**, 020401 (2003).

[9] X. Qian and W. Hübner, Phys. Rev. B **60**, 16192 (1999).

[10] H. Elmers, J. Hauschild, and U. Gradmann, J. Magn. Magn. Mater. **221**, 219 (2000).

[11] The public domain OOMMF package is available at http://math.nist.gov/oommf/

[12] H. Kronmüller and M. Fähnle, *Micromagnetism and the Microstructure of Ferromagnetic Solids* (University Press, Cambridge, 2003), p. 17.

[13] A. Kubetzka, Ph.D., 2002.

[14] A. Liechtenstein, M. Katsnelson, and V. Gubanov, J. Phys. F **14**, L125 (1984).

[15] A. Liechtenstein, M. Katsnelson, V. Antropov, and V. Gubanov, J. Magn. Magn. Mater. **67**, 65 (1987).

[16] E. Vedmedenko, H. Oepen, A. Ghazali, J.-C. Lévy, and J. Kirschner, Phys. Rev. Lett. **84**, 5884 (2000).

[17] S. Frota-Pessôa, R. Muniz, and J. Kudrnovský, Phys. Rev. B **62**, 5293 (2000).

[18] M. Pajda, J. Kudrnovský, I. Turek, V. Drchal, and P. Bruno, Phys. Rev. Lett. **85**, 5424 (2000).

[19] O. Mryasov, A. Freeman, and A. Liechtenstein, J. Appl. Phys. **79**, 4805 (1996).

[20] M. Hatherly, K. Hirakawa, R. Lowde, J. Mallett, M. Stringfellow, and B. Torrie, Proc. Phys. Soc. London **84**, 55 (1965).

[21] Q. Pankhurst, L. Barquin, J. Wicks, R. McGreevy, and M. Gibbs, J. Phys. Condens. Matter **9**, L375 (1997).

[22] K. Gallagher, M. Willard, V. Zabenkin, D. Laughlin, and M. McHenry, J. Appl. Phys. **85**, 5130 (1999).

[23] R. Muniz and D. Mills, Phys. Rev. B **66**, 174417 (2002).

[24] R. Muniz, A. Costa, and D. Mills, J. Phys. Condens. Matter **15**, S495 (2003).

[25] S. Chikazumi, *Physics of Ferromagnetism* (Oxford University Press, Oxford, 1999).

[26] R. Feyerherm, A. Loose, and J. Manson, J. Phys. Condens. Matter **15**, 663 (2003).